

Dysbiosis Contributes to Arthritis Development via Activation of Autoreactive T Cells in the Intestine

Yuichi Maeda,¹ Takashi Kurakawa,² Eiji Umemoto,¹ Daisuke Motooka,² Yoshinaga Ito,³ Kazuyoshi Gotoh,⁴ Keiji Hirota,⁵ Masato Matsushita,⁶ Yoki Furuta,¹ Masashi Narazaki,² Noriko Sakaguchi,² Hisako Kayama,¹ Shota Nakamura,² Tetsuya Iida,² Yukihiko Saeki,⁶ Atsushi Kumanogoh,¹ Shimon Sakaguchi,⁷ and Kiyoshi Takeda¹

Objective. The intestinal microbiota is involved in the pathogenesis of arthritis. Altered microbiota composition has been demonstrated in patients with rheumatoid arthritis (RA). However, it remains unclear how dysbiosis contributes to the development of arthritis. The aim of this study was to investigate whether altered composition of human intestinal microbiota in RA patients contributes to the development of arthritis.

Methods. We analyzed the fecal microbiota of patients with early RA and healthy controls, using 16S ribosomal RNA–based deep sequencing. We inoculated fecal samples from RA patients and healthy controls into germ-free arthritis-prone SKG mice and evaluated the immune responses. We also analyzed whether the lymphocytes of SKG mice harboring microbiota from RA patients

react with the arthritis-related autoantigen 60S ribosomal protein L23a (RPL23A).

Results. A subpopulation of patients with early RA harbored intestinal microbiota dominated by *Prevotella copri*; SKG mice harboring microbiota from RA patients had an increased number of intestinal Th17 cells and developed severe arthritis when treated with zymosan. Lymphocytes in regional lymph nodes and the colon, but not the spleen, of these mice showed enhanced interleukin-17 (IL-17) responses to RPL23A. Naive SKG mouse T cells cocultured with *P copri*–stimulated dendritic cells produced IL-17 in response to RPL23A and rapidly induced arthritis.

Conclusion. We demonstrated that dysbiosis increases sensitivity to arthritis via activation of autoreactive T cells in the intestine. Autoreactive SKG mouse T cells are activated by dysbiotic microbiota in the intestine, causing joint inflammation. Dysbiosis is an environmental factor that triggers arthritis development in genetically susceptible mice.

Supported by grants (to Dr. Takeda) from the Ministry of Education, Culture, Sports, Science and Technology, the Japan Agency for Medical Research and Development, and the Practical Research Project for Rare/Intractable Diseases, Japan Agency for Medical Research and Development.

¹Yuichi Maeda, MD, Eiji Umemoto, PhD, Yoki Furuta, MD, Hisako Kayama, PhD, Atsushi Kumanogoh, MD, PhD, Kiyoshi Takeda, MD, PhD: Osaka University, Osaka, Japan, and Japan Agency for Medical Research and Development, Tokyo, Japan; ²Takashi Kurakawa, PhD, Daisuke Motooka, PhD, Masashi Narazaki, MD, PhD, Noriko Sakaguchi, MD, PhD, Shota Nakamura, PhD, Tetsuya Iida, PhD: Osaka University, Osaka, Japan; ³Yoshinaga Ito, MD, PhD: Kyoto University, Kyoto, Japan; ⁴Kazuyoshi Gotoh, PhD: Osaka University, Osaka, Japan, and Okayama University Graduate School of Medicine, Okayama, Japan; ⁵Keiji Hirota, MD, PhD: Kyoto University, Kyoto, Japan, and Osaka University, Osaka, Japan; ⁶Masato Matsushita, MD, PhD, Yukihiko Saeki, MD, PhD: National Hospital Organization Osaka Minami Medical Center, Osaka, Japan; ⁷Shimon Sakaguchi, MD, PhD: Japan Agency for Medical Research and Development, Tokyo, Japan, Kyoto University, Kyoto, Japan, and Osaka University, Osaka, Japan.

Address correspondence to Kiyoshi Takeda, MD, PhD, Laboratory of Immune Regulation, Department of Microbiology and Immunology, Graduate School of Medicine, WPI Immunology Frontier Research Center, Osaka University, Suita, Osaka 565-0871, Japan. E-mail: ktakeda@ongene.med.osaka-u.ac.jp.

Submitted for publication November 26, 2015; accepted in revised form June 2, 2016.

Rheumatoid arthritis (RA) is a common autoimmune disease characterized by chronic synovitis and progressive destruction of cartilage and bone in multiple joints (1). In recent years, there has been rapid progress in the treatment of RA, with advances in the understanding of the molecular pathways involved (2,3). However, the etiology of RA is not fully understood.

Recent advances in genome-wide association studies and subsequent meta-analyses led to the identification of many alleles that govern RA susceptibility (4,5). However, the etiology of RA cannot be fully explained by these genetic factors, and many environmental factors are proposed to be involved in the disease onset (6). These environmental factors include smoking, hormones, and infection, and the

intestinal microbiota was recently shown to be critically involved in the induction of the disease, using several mouse models.

SKG mice, which bear a point mutation in the ZAP-70 gene (*Zap70*), spontaneously develop Th17 cell-dependent arthritis in a conventional facility (7). When reared in a specific pathogen-free (SPF) facility, SKG mice remain healthy until they are exposed to environmental agents such as fungi (8). In mice on the SKG genetic background, T cells with autoreactive T cell receptors (TCRs) are generated due to defective T cell selection in the thymus, and microbial stimulation of innate immunity induces activation of these autoreactive T cells, leading to arthritis development. However, SKG mice reared under germ-free conditions do not develop arthritis, even after treatment with fungal components, which indicates the possible involvement of intestinal microbiota in disease onset (9).

Additionally, HLA-B27-transgenic rats, which spontaneously develop spondyloarthritis, intestinal inflammation, and joint inflammation, do not show any signs of inflammation when they are raised in a germ-free facility (10). Mice lacking the interleukin-1 receptor antagonist (*IL-1Ra*^{-/-} mice) develop T cell-mediated arthritis in a SPF facility but not in a germ-free environment (11). In another model of arthritis, the K/BxN TCR-transgenic mouse, development of arthritis is initiated by the transgenic TCR recognizing glucose-6-phosphate isomerase. These transgenic mice do not exhibit any sign of joint inflammation when reared under germ-free conditions (12). In germ-free *IL-1Ra*^{-/-} mice or germ-free K/BxN mice, monocolonization with *Lactobacillus bifidus* or segmented filamentous bacteria (SFB) in the intestine, respectively, resulted in the induction of arthritis (11,12). Thus, a variety of mouse models of arthritis have shown that intestinal microbiota contributes to the onset of arthritis. However, the involvement of human microbiota in RA pathogenesis remains unknown.

In RA patients, an altered composition of intestinal microbiota (called dysbiosis) has been shown (13,14). Another study demonstrated the expansion of *Prevotella copri* in patients with new-onset RA in the US (15). The dysbiotic condition was partially resolved when RA disease improved upon treatment (14). Thus, similar to other diseases, such as inflammatory bowel disease, obesity, and diabetes, RA is correlated with dysbiosis (16). However, it remains unclear whether dysbiosis in RA patients causes disease onset.

In this study, we investigated whether the altered composition of human intestinal microbiota in RA patients can trigger the development of arthritis. Certain RA patients had microbiota markedly dominated by *Prevotellaceae*. SKG mice harboring microbiota from RA

patients had an increased number of intestinal Th17 cells and developed severe arthritis when treated with zymosan. Lymphocytes in regional lymph nodes and the large intestine, but not the spleen, of SKG mice harboring RA microbiota showed enhanced IL-17 production in response to the arthritis-related autoantigen 60S ribosomal protein L23a (RPL23A). Transfer of naive SKG mouse T cells cocultured with *P copri*-stimulated dendritic cells (DCs) led to an enhanced IL-17 response by T cells to RPL23A and rapid induction of arthritis in immunocompromised mice. These results suggest that *Prevotellaceae*-dominant intestinal microbiota is an environmental factor that promotes genetically susceptible T cells to induce arthritis.

PATIENTS AND METHODS

Patients and healthy controls. Fecal samples were obtained from 17 patients with early RA at National Hospital Organization Osaka Minami Medical Center and NTT West Osaka Hospital. Fecal samples from 14 healthy controls were collected by personnel at the Laboratory of Immune Regulation, Osaka University. The clinical characteristics of both groups are shown in Supplementary Table 1 (available on the *Arthritis & Rheumatology* web site at <http://onlinelibrary.wiley.com/doi/10.1002/art.39783/abstract>).

The inclusion criteria for RA patients were as follows: no previous treatment with disease-modifying antirheumatic drugs, biologic agents, or glucocorticoids (nonsteroidal antiinflammatory drugs were allowed), duration of RA not longer than 2 years, and a diagnosis of RA according to the American College of Rheumatology/European League Against Rheumatism 2010 criteria for RA (17). Exclusion criteria for both groups were as follows: extreme diets (e.g., strict vegetarians), treatment with antibiotics for at least 3 months prior to sampling, and known history of malignancy or serious disease of the heart, liver, or kidney. Human fecal samples were collected after the subjects provided informed consent, in accordance with the Declaration of Helsinki and with approval from the local ethics committees of Osaka University Hospital, NHO Osaka Minami Medical Center, and NTT West Osaka Hospital.

Extraction of bacterial DNA. Human and murine fecal samples were collected in tubes containing RNAlater (Ambion). After the weights of the samples were measured, RNAlater was added to make 10-fold dilutions of homogenates. Homogenates (200 μ l) were washed twice with 1 ml phosphate buffered saline and stored at -30°C until used. Bacterial DNA was extracted according to a previously described method (18). Briefly, 300 μ l of sodium dodecyl sulfate-Tris solution, 0.3g glass beads (diameter 0.1 mm) (BioSpec), and 500 μ l EDTA-Tris-saturated phenol were added to the suspension, and the mixture was vortexed vigorously using a FastPrep-24 (MP Biomedicals) at 5.0 power level for 30 seconds. After centrifugation at 20,000g for 5 minutes at 4°C , 400 μ l of supernatant was collected. Subsequently, phenol-chloroform extraction was performed, and 250 μ l of supernatant was subjected to isopropanol precipitation. Finally, DNAs were suspended in 200 μ l EDTA-Tris buffer and stored at -20°C .

Determination of microbiota by deep sequencing. Polymerase chain reaction (PCR) was performed using the primers

5'-AGGATTAGATACCCTGGTA-3' (784F) and 5'-CRRC ACGAGCTGACGAC-3' (1061R), which target the V5–V6 region of the 16S rRNA genes of bacteria (19), with KAPA HiFi HotStart ReadyMix (Kapa Biosystems). Products were purified using DNA Clean & Concentrator-5 (Zymo Research). Libraries were prepared using an Ion Fragment Library Kit (Life Technologies) according to the instructions of the manufacturer. Sequencing was performed using an Ion 318 Chip and Ion PGM Sequencing 400 Kit (Life Technologies) on an Ion PGM sequencer (Life Technologies). Raw sequences were demultiplexed and quality-trimmed according to the following procedures: 1) trimming bases with quality below Q15 from the 3' end of each read, 2) removing reads with average quality below Q20, 3) removing reads without primer sequences on both ends, and 4) removing reads with length shorter than 260 bp, using FASTX-Toolkit (http://hannonlab.cshl.edu/fastx_toolkit/index.html) and BBtrim (<http://bbmap.sourceforge.net/>). Five thousand reads in each sample were randomly selected using `random_sequence_sample.pl` (<https://www.ualberta.ca/~stothard/software.html>), and the selected data sets were used for further analysis. The processed sequences were then clustered into operational taxonomic units (OTUs) defined at 94% similarity cutoff using UCLUST version 1.2.22q (20). Representative sequences for each OTU were classified taxonomically using RDP Classifier version 2.2 (21) with the SILVA 111 database (22).

Clustering analysis. Clustering was performed according to the enterotyping tutorial provided by the European Molecular Biology Laboratory (<http://enterotype.embl.de/enterotypes.html>). Jensen–Shannon divergence (JSD) was calculated according to the relative genus abundances in each sample, by using the “`dist.JSD`” function coded in R. Based on the distance matrix, samples from 17 RA patients and 14 healthy controls were clustered by using the “`pam`” function in the R library “`cluster`.” The optimal number of clusters for the data sets was chosen by maximizing the Calinski–Harabasz index (“`index.G1`” function in the R library “`clusterSim`”). The result of clustering was visualized on a principal components analysis plot, using the `ade4` package in R.

Quantitative PCR (qPCR) of bacterial 16S rRNA genes. Quantitative PCR was performed in a StepOnePlus Real-time PCR System (Life Technologies) using GoTaq qPCR Master Mix (Promega). Amplification conditions were as follows: 94°C (5 minutes), 40 cycles of 94°C (20 seconds), 55°C (20 seconds), and 72°C (50 seconds). The following primer set targeting bacterial 16S rRNA was used: *Prevotella*, forward 5'-CACRGTAACGA TGGATGCC-3' and reverse 5'-GGTCGGGTTGCAGACC-3' (23). The data obtained by qPCR were expressed as the logarithm of the bacterial number per 1 gm of feces.

Mice. BALB/c and CB17/SCID mice were obtained from Clea. SKG mice and *rag-2*^{-/-} mice on the BALB/c background were described previously (7,24) and were maintained under SPF or germ-free conditions until inoculated with human microbiota. All animal experiments were performed in accordance with the guidelines of the Osaka University Animal Experimentation Committee.

Colonization of human fecal microbiota and induction of arthritis. Fresh human feces from 3 RA patients in cluster 4 (RA12, RA16, and RA17) harboring a high abundance of *Prevotellaceae*, 3 RA patients in cluster 2 (RA13, RA14, and RA15), 3 healthy controls in clusters 1 and 3 (HC2, HC10, and HC13), and 3 healthy controls in cluster 2 (HC5, HC7, and HC11), respectively, were collected and mixed. The feces were

homogenized in anaerobic resuspension buffer (2% Lab–Lemco powder, 0.1% L-cysteine, 0.045% KH₂PO₄, 0.09% NaCl, 0.045% (NH₄)₂SO₄, 0.0045% CaCl₂, 0.0045% MgSO₄ and 40% glycerol in 1,000 ml) at 16-fold dilution (weight/volume) and kept at –80°C until used. Female germ-free SKG mice (4–6 weeks old) were orally inoculated with 250 μ l of the fecal suspensions from RA patients or healthy controls and maintained in separate gnotobiotic isolators. Microbiota composition of the feces from mice at 20 weeks after the transfer was analyzed by deep sequencing. The bacterial counts of *Prevotella* and *Bacteroides* were also analyzed by qPCR of bacterial 16S rRNA genes in each mouse at 4–8 weeks after the fecal transfer, and mice with bacterial counts similar to those in human feces were used for the experiments. In some experiments, mice were intraperitoneally injected with zymosan (0.5 mg) at 5 weeks after the bacterial inoculation.

Isolation of lymphocytes and myeloid cells. To prepare lymphocytes from the spleen and regional lymph nodes, tissues were gently squeezed between glass slides, and the cells were passed through a 40- μ m nylon mesh. Intestinal lamina propria lymphocytes and myeloid cells were prepared as described previously (25). Briefly, the intestines were opened, washed to remove the fecal content, and then shaken in Hanks' balanced salt solution containing 5 mM EDTA for 20 minutes at 37°C. After removal of epithelial layers and fat tissue, the intestines were cut into small pieces and incubated with RPMI 1640 containing 4% fetal bovine serum, 1 mg/ml collagenase D (Roche), 0.5 mg/ml Dispase (Life Technologies), and 40 μ g/ml DNase I (Roche) for 50 minutes at 37°C in a shaking water bath. Lymphocytes were further enriched by Percoll density-gradient (40%/80%) centrifugation.

Antibodies and reagents. PerCP–Cy5.5–conjugated anti-CD4 (GK1.5), fluorescein isothiocyanate (FITC)–conjugated anti–interferon- γ (anti-IFN γ) (XMG1.2), allophycocyanin (APC)–conjugated anti–IL-17A (GK1.5), APC-conjugated anti-CD4 (GK1.5), phycoerythrin (PE)–Cy7–conjugated anti-CD62L (MEL-14), Pacific Blue–conjugated anti-CD44 (IM7), PE-conjugated anti-CD11b (M1/70), Pacific Blue–conjugated anti-CD45 (30-F11), APC-conjugated anti-mouse α 4 β 7 integrin (LPAM-1; DATk32), and purified anti-mouse CD3 ϵ (145-2C11) were purchased from BioLegend. APC-conjugated anti-CD11c (HL3) and APC-conjugated anti-CD16/CD32 (2.4G2) were purchased from BD Biosciences. Anti-FoxP3 (3G3) was purchased from Tonbo Biosciences. Anti-CD4 (L3T4) MicroBeads were purchased from Miltenyi Biotec. Zymosan A was purchased from Sigma-Aldrich.

Antibiotic treatment. Female SKG mice (4–6 weeks old) housed in the SPF facility were treated with or without antibiotics (1 gm/liter ampicillin, 0.5 gm/liter vancomycin, 1 gm/liter neomycin, and 1 gm/liter metronidazole) in drinking water. One week later, the mice were intraperitoneally injected with zymosan (5 mg).

Adoptive transfer. Splenic CD4⁺ T cells from 6–8-week-old germ-free SKG mice were isolated using a magnetic-activated cell sorting (MACS) system (Miltenyi Biotec) according to the instructions of the manufacturers. CD4⁺ T cells (5×10^5) were intravenously transferred to *rag-2*^{-/-} mice reared in the SPF facility.

Clinical assessment of arthritis. Joint swelling was monitored by inspection and was scored as follows: 0 = no joint swelling, 0.1 = swelling of 1 finger joint, 0.5 = mild swelling of wrist or ankle, and 1.0 = severe swelling of wrist or ankle. Scores for all fingers of the fore paws and hind paws, wrists, and ankles

were totaled for each mouse. Ankle thickness was measured using a dial thickness gauge (G-1A; Ozaki).

Flow cytometry. The intracellular expression of IFN γ and IL-17 in CD4⁺ T cells was analyzed using a Cytotfix/Cytoperm Kit Plus (BD Biosciences) according to the manufacturer's instructions. Lymphocytes were incubated with 50 ng/ml phorbol myristate acetate (Sigma), 5 μ M calcium ionophore A23187 (Sigma), and GolgiStop in complete RPMI 1640 at 37°C for 4 hours. Surface staining was performed with PerCP-Cy5.5-conjugated anti-CD4 monoclonal antibodies (mAb) (2 μ g/ml). After Fix/Perm treatment for 20 minutes, intracellular cytokine staining was performed with FITC-conjugated anti-IFN γ (5 μ g/ml) and APC-conjugated anti-IL-17A (5 μ g/ml) mAb for 20 minutes. For FoxP3 staining, a FoxP3 Staining Buffer Set (eBioscience) was used.

Data were acquired using a FACSCanto II system (BD Biosciences). To measure the absolute number of CD4⁺ T cells, the total number of cells isolated from the tissues was counted, and the proportion of each cell population was evaluated by flow cytometry. The number of CD4⁺ T cells was calculated as total cell number \times percentage as determined by flow cytometry. Because the protocols for analysis of IFN γ -positive or IL-17-positive CD4⁺ T cells and those for analysis of FoxP3-positive T cells were different, we analyzed these populations independently.

Histologic analysis, radiographic observation, and enzyme-linked immunosorbent assay (ELISA) for autoantibodies. Ankle joints were fixed with a 4% paraformaldehyde-phosphate buffer solution, and paraffin-embedded sections were stained with hematoxylin and eosin (H&E). Images were obtained using a BZ-9000 microscope (Keyence). The severity of inflammation in ankle joints was scored as follows: 0 = none, 1 = mild, 2 = moderate, and 3 = severe. Computed tomography (CT) scanning of the ankle joints was performed using a 3-dimensional x-ray micro-CT imager for laboratory animals (Rigaku). The serum concentration of rheumatoid factor (RF) was analyzed using an IgG rheumatoid factor mouse ELISA kit (Shibayagi) according to the manufacturer's instructions.

Cytokine production of CD4⁺ T cells in popliteal lymph nodes. CD4⁺ T cells from popliteal lymph nodes were isolated using MACS (Miltenyl Biotec) according to the manufacturer's instructions. Subsequently, 1.2×10^5 CD4⁺ T cells were stimulated with 1 μ g/ml anti-CD3 antibody for 24 hours. Cytokine production in the supernatants was analyzed by ELISA (R&D Systems).

Evaluation of RPL23A-reactive T cells. Recombinant mouse RPL23A fused with glutathione S-transferase (GST) was prepared as described previously (26). Lymphocytes were isolated from the regional lymph nodes (brachial, axillary, inguinal, and popliteal), large intestine, small intestine, and spleen 4 weeks after inoculation with human microbiota. Lymphocytes from the regional lymph nodes and large intestine of 8-week-old germ-free SKG mice were also isolated. Cells (5×10^5) were cultured with 50 μ g/ml of RPL23A-GST or GST for 48 hours. Concentrations of IL-17A and IFN γ in the culture supernatants were analyzed by ELISA (R&D Systems) according to the manufacturer's instructions.

Bacterial culture. *P copri* JCM 13464^T, *Bacteroides fragilis* JCM 11019^T, *Bifidobacterium bifidum* JCM 1209^T, *Lactobacillus acidophilus* JCM 1132^T, or *Escherichia coli* JCM 1649^T

were cultured in Gifu anaerobic medium (GAM) Broth (Nissui Pharmaceutical) under anaerobic conditions. Bacterial suspensions were washed with cell culture medium, and the optical density at 600 nm was measured to estimate bacterial numbers. Bacterial numbers were determined microscopically with DAPI staining (Vector). Bacteria were heat-killed (90°C for 30 minutes) for further experiments.

Activation of autoreactive T cells. Bone marrow-derived dendritic cells (BMDCs) (2×10^5) prepared from BALB/c mice were incubated with 2×10^6 heat-killed *P copri*, *B fragilis*, *B bifidum*, *L acidophilus*, or *E coli* for 24 hours. Splenic naive CD4⁺ T cells (CD4⁺CD62L^{high}CD44^{low} cells) from 6–8 week-old SKG or BALB/c mice were sorted with GAM broth (Nissui Pharmaceutical), and 7×10^5 cells were cocultured with 5×10^4 bacteria-stimulated DCs for 4 days. T cells (5×10^4) were then restimulated with irradiated splenocytes (2.5×10^4) from BALB/c mice in the presence of recombinant RPL23A-GST or GST (5 μ g/ml). Two days later, the culture supernatant was harvested for ELISA to evaluate cytokine production.

Analysis of IL-6 production in myeloid cell subsets. CD11b⁻ DCs, CD11b⁺CD11c⁺ cells, and CD11b⁺ macrophages in the large intestine were isolated 8 weeks after the inoculation with human microbiota, using a FACSaria instrument. Total RNA was isolated from myeloid cell subsets and reverse transcribed. Complementary DNA was analyzed by real-time reverse transcription-PCR. Values were normalized to the expression of GAPDH, and the fold difference in expression relative to that of GAPDH was determined. The following primer sets were used: IL-6, forward 5'-CTGCAAGAGACTTCCATCCAGTT-3' and reverse 5'-AAGTAGGGAAGGCCGTGGTT-3'; GAPDH, forward 5'-TGGATATTGTTGCCATCAATG-3' and reverse 5'-TGATGGGATTTCCATTGATGA-3'.

Stimulation of BMDCs. BMDCs (2×10^5) prepared from BALB/c mice were stimulated with heat-killed *P copri*, *B fragilis*, *B bifidum*, *L acidophilus*, or *E coli* (1×10^4 or 1×10^5 ; DC-to-bacterium ratio 1:0.05 or 1:0.5) for 12 hours. In some experiments, BMDCs were stimulated with a mixture of heat-killed fecal samples from 3 RA patients (RA12, RA16, and RA17) or 3 healthy controls (HC2, HC10, and HC13) at a DC-to-bacterium ratio of 1:0.6 or 1:0.3. The cytokine concentration in the supernatants was analyzed by ELISA (R&D Systems).

Generation of *P copri*-monocolonized SKG mice. Germ-free SKG mice (4–6 weeks old) were orally inoculated with or without pure preparations of cultured 1×10^8 *P copri* JCM 13464^T and maintained in separate gnotobiotic isolators. These mice were intraperitoneally injected with zymosan (0.5 mg) at 5 weeks after the bacteria inoculation. The arthritis score and ankle thickness were monitored for 8 weeks after the injection. Immune cell populations were analyzed by flow cytometry at 8 weeks after the injection.

Transfer of SKG mouse T cells cocultured with bacteria-stimulated DCs. Splenic naive CD4⁺ T cells from SKG mice were cocultured with BMDCs stimulated with heat-killed bacteria (*P copri* or *B fragilis*) as described above. After 4 days, 1×10^5 T cells were transferred intravenously into SCID mice.

Transfer of SKG mouse CD4⁺ T cells isolated from the large intestine or spleen. CD4⁺ T cells were isolated from the large intestine or spleen of 8-week-old SKG mice reared in the SPF facility, by using a MACS system (Miltenyl Biotec) according to the manufacturer's instructions. The purity of CD4⁺ T cells was >95%. CD4⁺ T cells (1×10^5) were intravenously transferred to SCID mice reared in the SPF facility.

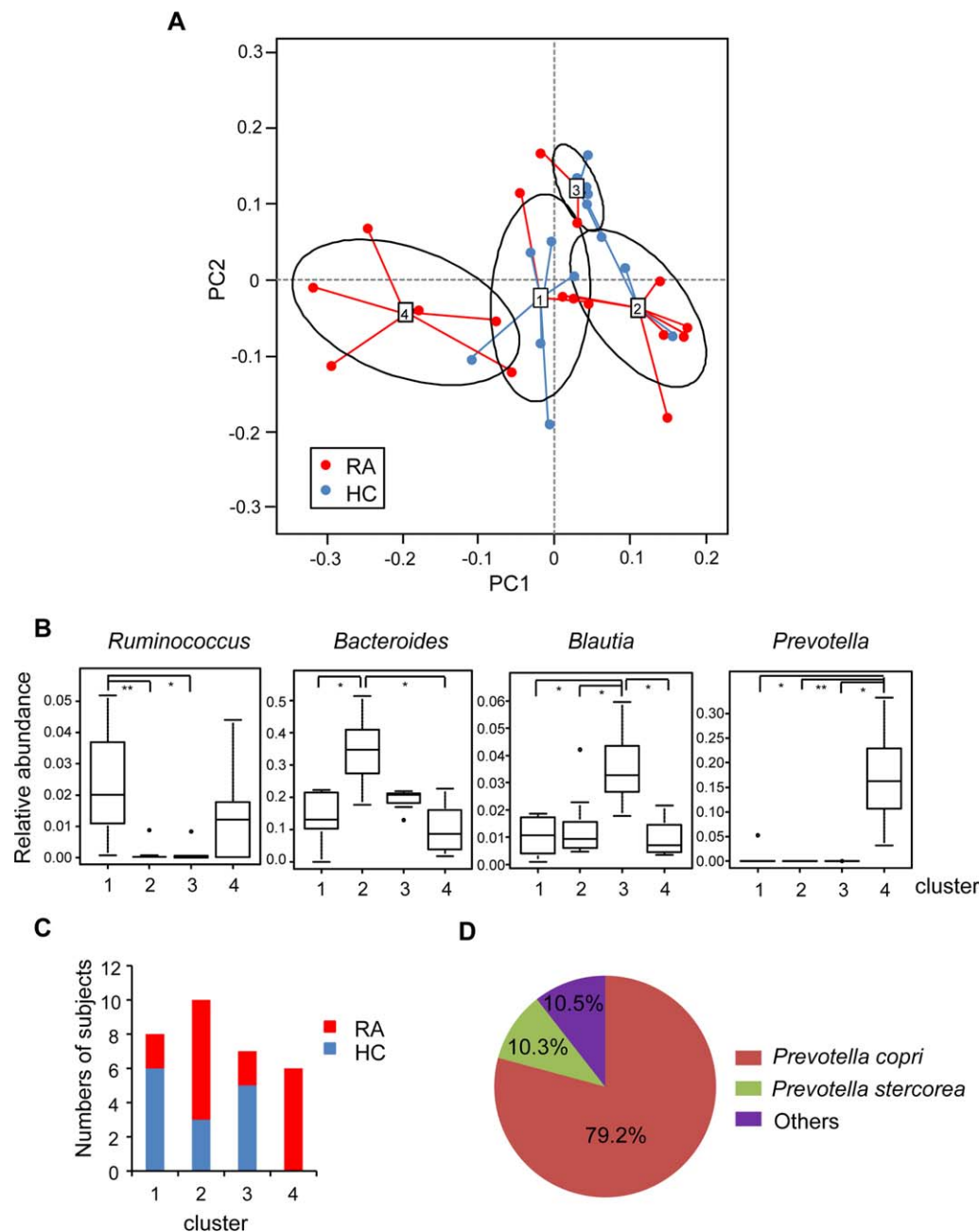


Figure 1. Dysbiosis in certain patients with rheumatoid arthritis (RA). **A**, Clustering of 17 RA patients and 14 healthy controls (HCs) shown on a principal components analysis plot; a clustering analysis was performed at the genus level. **B**, Bacterial composition in the 4 clusters. Data are presented as box plots, where the boxes represent the 25th to 75th percentiles, the lines within the boxes represent the median, and the lines outside the boxes represent the 10th and 90th percentiles. Circles indicate outliers. Mann-Whitney U tests were conducted, and the Bonferroni correction was applied to adjust for multiple comparisons. * = $P < 0.05$; ** = $P < 0.01$. **C**, Distribution of RA patients and HCs in each cluster. **D**, Composition of operational taxonomic units assigned to *Prevotella* in the 6 RA patients in cluster 4. The partial ribosomal RNA sequences assigned to *Prevotella* by deep sequencing were analyzed with BLAST (online at www.nlm.nih.gov).

SCID mice started oral treatment with a cocktail of antibiotics (1 gm/liter ampicillin, 0.5 gm/liter vancomycin, 1 gm/liter neomycin, and 1 gm/liter metronidazole) 7 days before the CD4+ T cell transfer and continued to be treated during the experiments. Popliteal lymph node cells were prepared from the

SCID mice 8 weeks after the transfer and analyzed for $\alpha 4\beta 7$ integrin-positive CD4+ T cells by flow cytometry.

Statistical analysis. Data are expressed as the mean \pm SD. The arthritis scores, ankle thickness, histologic scores, and immune cell populations were analyzed by Mann-Whitney U test.

To assess significant differences in the relative abundance of specific genera as assessed by the microbiota analysis, Mann-Whitney U tests were conducted, with Bonferroni adjustment for multiple comparisons. In other experiments, differences between 2 groups were evaluated by Student's unpaired *t*-test. The multiple comparisons were evaluated by one-way analysis of variance with Tukey's test.

RESULTS

Altered composition of fecal microbiota in certain RA patients. We analyzed the microbiota of feces obtained from 17 patients with early RA who were not treated with antirheumatic drugs and 14 healthy controls, by using 16S rRNA-based deep sequencing (see Supplementary Table 1, available on the *Arthritis & Rheumatology* web site at <http://onlinelibrary.wiley.com/doi/10.1002/art.39783/abstract>).

The clustering analysis at the genus level showed that all of the samples were clustered into 1 of 4 clusters (Figure 1A and Supplementary Figure 1, available on the *Arthritis & Rheumatology* web site at <http://onlinelibrary.wiley.com/doi/10.1002/art.39783/abstract>). Each cluster was characterized by a high abundance of the following genera: *Ruminococcus* in cluster 1, *Bacteroides* in cluster 2, *Blautia* and *Faecalibacterium* in cluster 3, and *Prevotella* in cluster 4 (Figure 1B and Supplementary Figure 2, available on the *Arthritis & Rheumatology* web site at <http://onlinelibrary.wiley.com/doi/10.1002/art.39783/abstract>). Cluster 4 was composed of only RA patients, whereas the other clusters included both RA patients and healthy controls (Figure 1C), indicating that *Prevotella* is a candidate involved in RA pathogenesis.

Among the OTUs that were assigned to *Prevotella* in cluster 4, the majority (79.2%) showed a high (>99%) similarity to *P copri* (accession no. NR_113411.1), followed by 10.3% of OTUs to *Prevotella stercorea* (accession no. NR_041364.1) (Figure 1D). Based on rarefaction analysis, the trend of species richness in cluster 4 was similar to that in other clusters (see Supplementary Figure 3, available on the *Arthritis & Rheumatology* web site at <http://onlinelibrary.wiley.com/doi/10.1002/art.39783/abstract>). Quantitative PCR analysis showed that the bacterial counts of *Prevotella* in RA patients in cluster 4 were markedly higher than those in other RA patients and healthy controls (see Supplementary Table 2, available on the *Arthritis & Rheumatology* web site at <http://onlinelibrary.wiley.com/doi/10.1002/art.39783/abstract>). In RA patients in cluster 4, serum concentrations of C-reactive protein and matrix metalloproteinase 3 were relatively higher than those in RA patients in other clusters (see Supplementary Table 3, available on the *Arthritis & Rheumatology* web site at <http://onlinelibrary.wiley.com/doi/10.1002/art.39783/abstract>). Although RA patients in cluster 4 did not show any association with HLA-DRB1, they were all positive for RF and anti-citrullinated protein antibody (ACPA).

Colonization of SKG mice with human fecal microbiota. To analyze whether human intestinal bacteria contribute to arthritis development, we used SKG mice. Similar to a previous observation in germ-free SKG mice (9), SPF-housed SKG mice treated with a combination of antibiotics (ampicillin, vancomycin, neomycin, and metronidazole) did not develop arthritis after an intraperitoneal injection of zymosan (a fungal β -glucan) (see Supplementary Figure 4A, available on the *Arthritis & Rheumatology* web site at <http://onlinelibrary.wiley.com/doi/10.1002/art.39783/abstract>). In addition, T cells from germ-free SKG mice induced arthritis when transferred into *rag2*^{-/-} mice reared in an SPF facility, although the severity of arthritis was milder than that observed in *rag2*^{-/-} mice that received SPF-housed SKG mouse T cells (see Supplementary Figure 4B, available on the *Arthritis & Rheumatology* web site at <http://onlinelibrary.wiley.com/doi/10.1002/art.39783/abstract>). Thus, in addition to the fact that intestinal microbiota is involved in the pathogenesis of arthritis in SKG mice, SKG mouse T cells generated under the germ-free condition have an ability to induce arthritis in the presence of intestinal microbiota, indicating that the SKG mouse is an appropriate model for the analysis of intestinal microbiota and arthritis.

We inoculated a mixture of feces from 3 RA patients (RA12, RA16, and RA17 from cluster 4) and 3 healthy controls (HC2 and HC10 from cluster 3 and HC13 from cluster 1) into germ-free SKG mice (mice harboring microbiota from RA patients and mice harboring microbiota from healthy controls were referred to as RA-SKG and HC-SKG, respectively). The fecal microbiota analysis by deep sequencing showed that the abundance of *Prevotellaceae* (one of the dominant families in these RA patients) was ~25% in RA-SKG mice at 20 weeks after colonization, which was a level comparable with that in RA patients (Figures 2A and B). More than 80% of the OTUs assigned to *Prevotellaceae* in RA-SKG mice were identical to *P copri* (accession no. NR_113411.1) (Figure 2C). Additionally, the abundance of *Bacteroidaceae* (one of the dominant families in the feces of healthy controls) in HC-SKG mice was comparable to that observed in healthy control subjects. These results suggest that the fecal microbiota composition in RA patients and healthy controls was successfully reproduced in SKG mice.

We next analyzed the severity of arthritis in RA-SKG and HC-SKG mice reared in isolators for 20 weeks. No severe arthritis was observed in either group at 20 weeks after the fecal inoculation. Additionally, the mean arthritis scores and ankle thickness values were not statistically significantly different between the 2 groups (see Supplementary Figures 5A and B, available on the *Arthritis & Rheumatology* web site at <http://onlinelibrary.wiley.com/doi/10.1002/art.39783/abstract>). Thus, SKG mice harboring

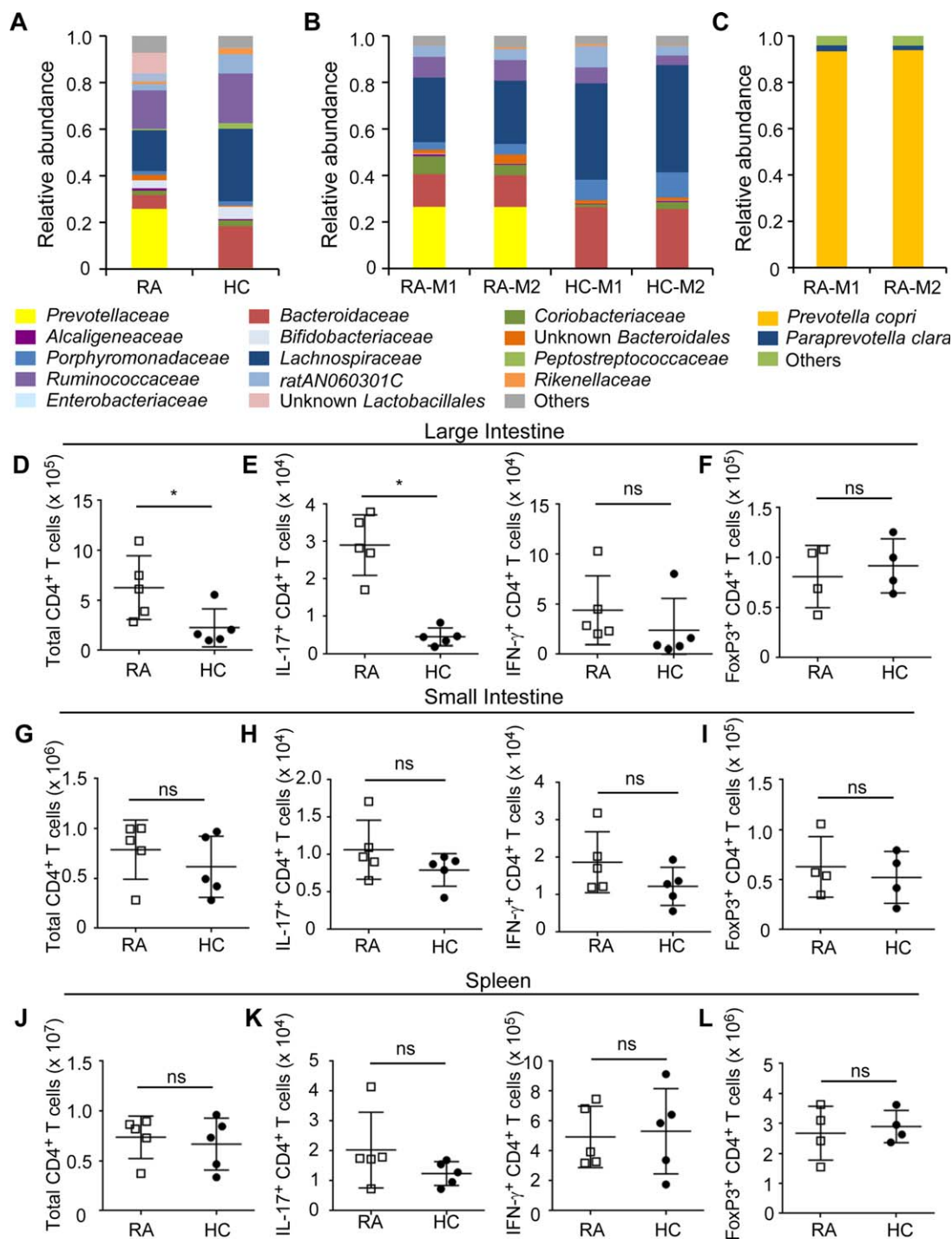


Figure 2. Generation of SKG mice colonized with human microbiota. **A**, Percentages of family-level bacterial composition in a mixture of feces from 3 rheumatoid arthritis (RA) patients and 3 healthy controls (HCs). **B**, Percentages of family-level bacterial composition in the feces of SKG mice harboring microbiota from RA patients (RA-SKG mice) (RA-M1 and RA-M2) and SKG mice harboring microbiota from healthy controls (HC-SKG mice) (HC-M1 and HC-M2) at 20 weeks after the inoculation. **C**, Percentages of *Prevotella copri*, *Paraprevotella clara*, and others in the family of *Prevotellaceae* in the feces of RA-SKG mice (RA-M1 and RA-M2). **D–L**, Flow cytometric analysis of immune cell populations in lamina propria lymphocytes and splenic cells prepared from RA-SKG and HC-SKG mice at 20 weeks after the inoculation. The numbers of total CD4⁺ T cells, interleukin-17-positive (IL-17⁺) CD4⁺ T cells, interferon- γ -positive (IFN γ ⁺) CD4⁺ T cells, and FoxP3⁺ CD4⁺ T cells in the large intestine (**D–F**), the small intestine (**G–I**), and spleen (**J–L**) are shown. Symbols represent individual mice; bars show the mean \pm SD. Data are representative of 3 independent experiments. * = $P < 0.05$. NS = not significant.

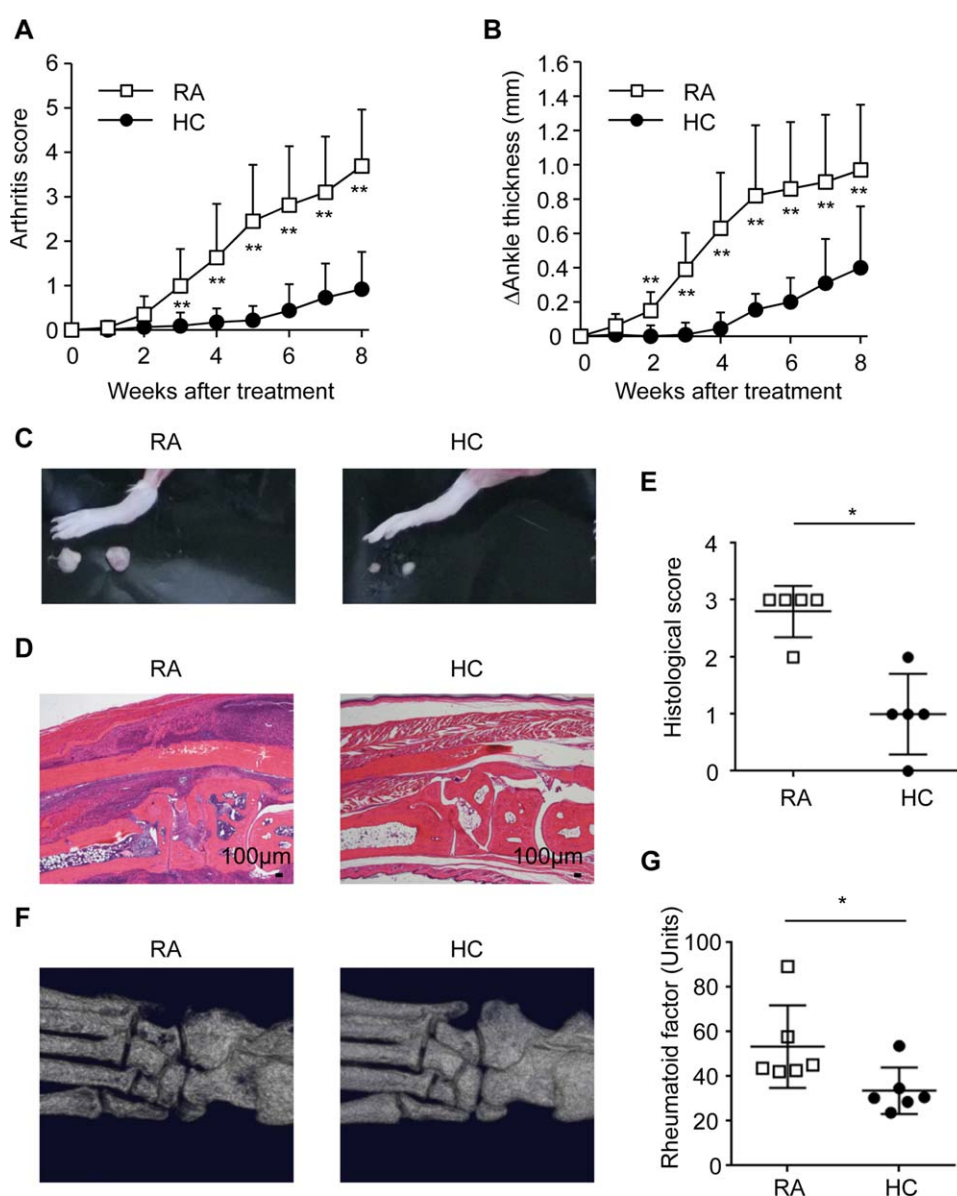


Figure 3. Severe arthritis in RA-SKG mice. Female germ-free SKG mice were inoculated with a mixture of fecal samples from 3 RA patients and 3 healthy controls and maintained in separate gnotobiotic isolators. Five weeks after the inoculation, the mice were intraperitoneally injected with 0.5 mg of zymosan and monitored for 8 weeks. **A** and **B**, Arthritis score (**A**) and change in ankle thickness (**B**) in RA-SKG mice ($n = 10$) and HC-SKG mice ($n = 11$) after the injection of zymosan. Each symbol and vertical lines represent the mean \pm SD. Results are from 2 independent experiments combined. **C**, Representative radiographic images showing joint swelling and popliteal lymph nodes in an RA-SKG mouse and an HC-SKG mouse. **D**, Representative histologic sections of ankle joints from an RA-SKG mouse and an HC-SKG mouse. **E**, Histologic scores for the ankle joints of RA-SKG mice and HC-SKG mice. **F**, Representative radiographic images of the ankle joints from an RA-SKG mouse and an HC-SKG mouse showing severe bone erosion in the RA-SKG mouse. **G**, Serum rheumatoid factor levels in RA-SKG mice and HC-SKG mice. Results shown in **C**–**G** were obtained at 8 weeks after the zymosan injection. Symbols represent individual mice; bars show the mean \pm SD. * = $P < 0.05$; ** = $P < 0.01$. See Figure 2 for definitions.

human microbiota did not develop arthritis spontaneously, as do SKG mice reared in an SPF facility.

We then used flow cytometry to analyze the number of immune cell populations 20 weeks after colonization with fecal microbiota. The total number of CD4⁺ T

cells and the number of IL-17–producing CD4⁺ T cells in the large intestine were increased in RA-SKG mice compared with HC-SKG mice (Figures 2D and E and Supplementary Figure 6A, available on the *Arthritis & Rheumatology* web site at <http://onlinelibrary.wiley.com/>

doi/10.1002/art.39783/abstract). However, the number of IFN γ + CD4+ T cells and FoxP3+ CD4+ T cells in the large intestine were not altered in RA-SKG mice (Figures 2E and F and Supplementary Figures 6A and B). The numbers of IL-17+, IFN γ +, or FoxP3+ CD4+ T cells in the small intestine and spleen were not different in the 2 groups (Figures 2G–L and Supplementary Figures 6C–F). These results indicate that RA patient–derived microbiota did not induce spontaneous arthritis development in mice at 20 weeks but had the potential to increase the number of Th17 cells in the large intestine.

Development of severe arthritis in RA microbiota–colonized SKG mice. A single injection of zymosan elicits the development of severe arthritis in SPF-housed SKG mice (8). Therefore, we evaluated the contribution of RA microbiota to arthritis development in SKG mice in the presence of zymosan. We injected a low dose of zymosan intraperitoneally into RA-SKG and HC-SKG mice at 5 weeks after colonization with microbiota. We monitored joint swelling in all digits, wrists, and ankles for 8 weeks after the zymosan injection. RA-SKG mice showed severe swelling in the joints (Figures 3A–C). Moreover, RA-SKG mice had marked hypertrophy of the popliteal lymph nodes (Figure 3C).

Histologic analysis of the ankle joints using H&E staining demonstrated that RA-SKG mice had severe synovitis and destruction of cartilage and bone compared with HC-SKG mice (Figures 3D and E). Additionally, radiography showed that RA-SKG mice had severe bone erosion (Figure 3F). RA-SKG mice developed high titers of RF (Figure 3G). We next investigated whether the microbiota of RA patients without *Prevotella* induces severe arthritis. Microbiota of RA patients in cluster 2 (a mixture of feces from RA13, RA14, and RA15) were colonized in germ-free–housed SKG mice, followed by injection with zymosan (see Supplementary Figures 7A and B, available on the *Arthritis & Rheumatology* web site at <http://onlinelibrary.wiley.com/doi/10.1002/art.39783/abstract>). These mice did not develop severe arthritis compared with RA-SKG mice, in which microbiota of RA patients in cluster 4 was colonized. In addition, microbiota of 3 healthy controls from cluster 2 (HC5, HC7, and HC11) did not induce severe arthritis (see Supplementary Figures 7A and B). Thus, RA-SKG mice harboring *Prevotella*-dominated microbiota developed severe arthritis after zymosan treatment.

We next evaluated the immune cell populations 3 weeks after the zymosan injection, when the mice did not show severe inflammatory change in the joints. Similar to the results observed without zymosan treatment (Figures 2D and E), the total number of CD4+ T cells and the number of IL-17+ CD4+ T cells were increased in the large

intestine (Supplementary Figures 8A and B, available on the *Arthritis & Rheumatology* web site at <http://onlinelibrary.wiley.com/doi/10.1002/art.39783/abstract>). In addition, the number of IL-17+ CD4+ T cells in popliteal lymph nodes was slightly, albeit not significantly, increased in RA-SKG mice (Supplementary Figures 8C and D). The numbers of IL-17+ or IFN γ + CD4+ T cells in the small intestine and spleen were unchanged, consistent with the finding that the total number of CD4+ T cells was not increased in these tissues (Supplementary Figures 8E–H).

We further analyzed the immune cell populations 8 weeks after zymosan treatment, when the RA-SKG mice showed severe arthritis. The numbers of total CD4+ T cells and IL-17+ CD4+ T cells in the large intestine and popliteal lymph nodes were markedly increased at 8 weeks (see Supplementary Figures 9A–D, available on the *Arthritis & Rheumatology* web site at <http://onlinelibrary.wiley.com/doi/10.1002/art.39783/abstract>). However, the numbers of IL-17+ CD4+ T cells in the small intestine and spleen were not changed (see Supplementary Figures 9E–H). Moreover, the production of IL-17A, but not IFN γ , by CD4+ T cells in popliteal lymph nodes stimulated with anti-CD3 antibody was increased in RA-SKG mice (see Supplementary Figures 10A and B, available on the *Arthritis & Rheumatology* web site at <http://onlinelibrary.wiley.com/doi/10.1002/art.39783/abstract>). Thus, the severe arthritis observed in RA-SKG mice correlated with enhanced Th17 cell responses.

Enhanced response to an arthritis-related autoantigen in RA microbiota–colonized SKG mice. We next investigated whether lymphocytes from RA-SKG mice show enhanced responses to the arthritis-related autoantigen RPL23A (26). Cells were isolated from the regional lymph nodes, intestine, and spleen of RA-SKG and HC-SKG mice at 4 weeks after microbiota colonization, stimulated with RPL23A or control GST protein, and analyzed by ELISA for production of IL-17A and IFN γ . RPL23A-induced production of IL-17A, but not IFN γ , in regional lymph node cells was higher in RA-SKG mice than in HC-SKG mice (Figures 4A and B). Furthermore, RPL23A-induced IL-17A IFN γ production, but not IFN γ production, in cells from the large intestine was also highly enhanced in RA-SKG mice compared with HC-SKG mice (Figures 4C and D). No significant difference in cytokine production in cells from the small intestine or spleen between RA-SKG mice and HC-SKG mice was observed (Figures 4E–H). Additionally, cells isolated from regional lymph nodes and the large intestine of germ-free–housed SKG mice did not show RPL23A-induced IL-17A production (Figures 4A–D). Thus, the high RPL23A-induced response of lymphocytes from regional

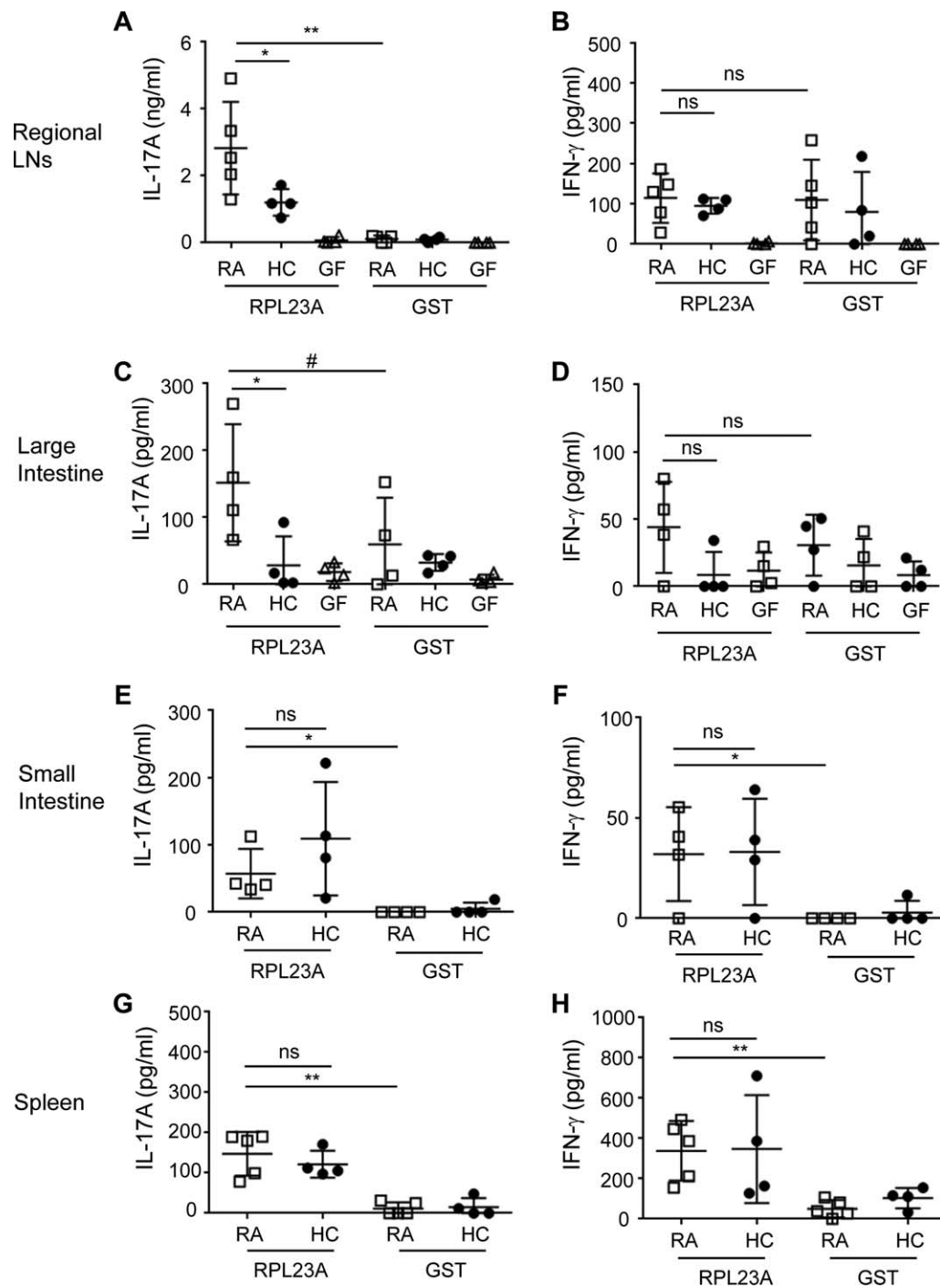


Figure 4. Autoantigen-reactive lymphocytes in RA-SKG mice and HC-SKG mice. Lymphocytes were isolated from the regional lymph nodes (LNs) (brachial, axillary, inguinal, and popliteal), large and small intestine, and spleen of RA-SKG and HC-SKG mice 4 weeks after the microbiota inoculation. Lymphocytes were also isolated from the regional lymph nodes and large intestine of germ-free (GF) SKG mice. **A, C, E, and G,** Interleukin-17A (IL-17A) production by lymphocytes stimulated with recombinant RPL23A or glutathione S-transferase (GST). **B, D, F, and H,** Interferon- γ (IFN γ) production by lymphocytes stimulated with recombinant RPL23A or GST. Symbols represent individual mice; bars show the mean \pm SD. Results are representative of 2 independent experiments. * = $P < 0.05$; ** = $P < 0.01$. NS = not significant (see Figure 2 for other definitions).

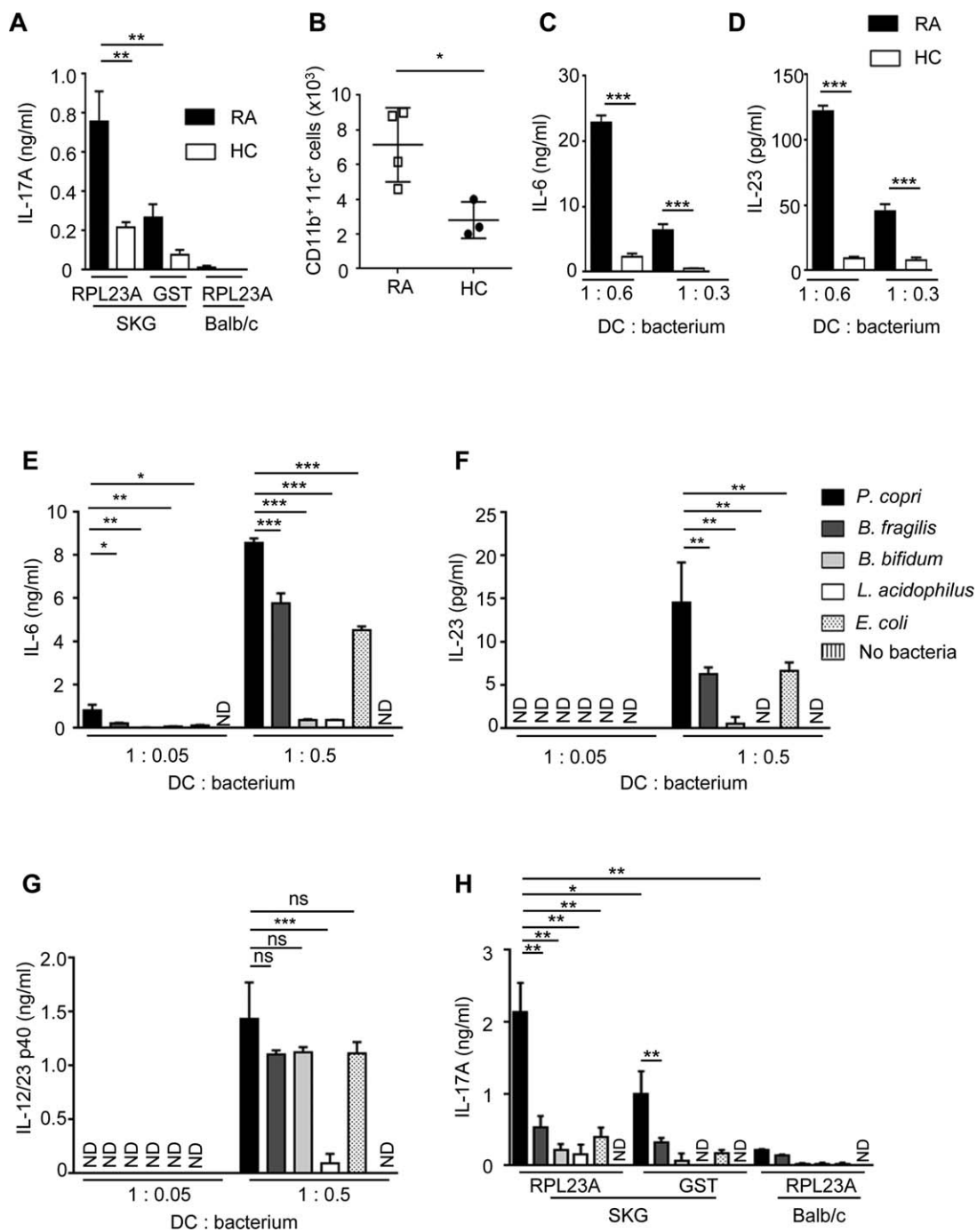


Figure 5. Activation of autoantigen-reactive SKG mouse T cells by *Prevotella copri*. **A**, Naive CD4⁺ T cells from SKG or BALB/c mice were cocultured with dendritic cells (DCs) stimulated with RA or healthy control microbiota. Cells were stimulated with RPL23A or glutathione S-transferase (GST), and the concentration of IL-17A was measured by enzyme-linked immunosorbent assay (ELISA). **B**, The numbers of CD45⁺CD11b⁺CD11c⁺ cells in the large intestine of RA-SKG and HC-SKG mice 8 weeks after the microbiota inoculation are shown. Symbols represent individual mice; bars show the mean \pm SD. **C–G**, Bone marrow-derived DCs were stimulated with RA or HC microbiota or the indicated heat-killed bacteria, and the production of IL-6 (**C** and **E**), IL-23 (**D** and **F**), and IL-12/23 p40 (**G**) was measured by ELISA. **H**, Naive CD4⁺ T cells from SKG or BALB/c mice were cocultured with DCs stimulated with the indicated heat-killed bacteria. Cells were stimulated with recombinant RPL23A or GST, and the concentration of IL-17A was measured by ELISA. Values in **A** and **C–H** are the mean \pm SD of triplicate measurements. All data are representative of at least 2 independent experiments. * = $P < 0.05$; ** = $P < 0.01$; *** = $P < 0.001$. NS = not significant; ND = not detected (see Figure 2 for other definitions).

lymph nodes and the large intestine was dependent on RA microbiota.

***P copri* augmentation of the T cell response to the arthritis-related autoantigen.** We hypothesized that naive CD4⁺ T cells from mice on the SKG genetic background are activated to show an enhanced response to the arthritis-related autoantigen RPL23A in the intestine by the *Prevotella*-dominated RA microbiota. Therefore, we examined whether SKG mouse T cells cocultured with RA microbiota-stimulated DCs react to RPL23A. To this end, BMDCs were first treated with a mixture of fecal samples from RA patients (*Prevotella*-dominated) or healthy controls, and naive splenic T cells from SKG or BALB/c mice were cocultured with the stimulated DCs for 4 days. The T cells were then cultured with RPL23A in the presence of antigen-presenting cells for 2 days. SKG mouse T cells that had been cultured with the RA microbiota-stimulated DCs produced IL-17A at high levels in response to RPL23A compared with T cells cultured with the healthy control microbiota-stimulated DCs (Figure 5A).

Because SKG mice develop arthritis via activation of innate immunity (8), we assessed the ability of *P copri*-dominated microbiota to bring about such activation of innate immune cells in vivo and in vitro. We first analyzed the number of CD11b⁺CD11c⁺ cells (which have been reported to induce Th17 cells and produce high levels of IL-6 compared with other innate immune subsets of cells) in the large intestine of RA-SKG and HC-SKG mice (25,27) (Supplementary Figures 11A and B). Both the frequency and number of CD11b⁺CD11c⁺ cells in the large intestine were increased in RA-SKG mice (Figure 5B and Supplementary Figures 11C and D, available on the *Arthritis & Rheumatology* web site at <http://onlinelibrary.wiley.com/doi/10.1002/art.39783/abstract>).

We next evaluated whether *Prevotella*-dominated RA microbiota has an ability to induce Th17 cell-related cytokines in vitro. BMDCs were stimulated with RA or healthy control microbiota and analyzed for the production of Th17 cell-related cytokines, such as IL-6 and IL-23 (Figures 5C and D). The RA microbiota induced production of higher levels of IL-6 and IL-23 than did healthy control microbiota. Thus, *Prevotella*-dominated RA microbiota induced enhanced activation of DCs and RPL23A-mediated Th17 responses.

We next investigated responses to pure preparations of the representative in vitro-cultured intestinal bacteria. BMDCs were cultured with *P copri*, *B fragilis*, *B bifidum*, *L acidophilus*, and *E coli* and analyzed for production of inflammatory cytokines such as IL-6, IL-23, and IL-12/23p40 by ELISA (Figures 5E–G). There was only marginal production of IL-6 and IL-23 by stimulation with *B bifidum*

and *L acidophilus*, while *P copri*-induced IL-6 production was higher than that induced by *B fragilis* and *E coli* at any bacterial ratio analyzed. Furthermore, at a DC-to-bacterium ratio of 1:0.5, *P copri* induced a markedly high level of IL-23 compared with that induced by other bacteria. IL-12/23p40 production was almost equivalently induced by *P copri*, *B fragilis*, *B bifidum*, and *E coli*, indicating that *P copri* possesses a unique ability to provoke Th17 cell-biased immune responses. We also analyzed T cell IL-17A production after coculture with DCs that were activated by intestinal bacteria (Figure 5H). SKG mouse T cells cocultured with *P copri*-stimulated DCs produced increased amounts of IL-17A in response to RPL23A compared with SKG mouse T cells cultured with other bacteria-stimulated DCs. However, BALB/c mouse T cells that had been cocultured with *P copri*-stimulated DCs did not produce IL-17A in response to RPL23A. Taken together, these findings suggest that *P copri* exhibits a potent ability to induce Th17 cell-related cytokines, leading to enhanced RPL23A-dependent Th17 cell responses in SKG mouse T cells.

Because *P copri* was shown to induce RPL23A-mediated Th17 cell responses in vitro, we next investigated whether monocolonization of *P copri* in SKG mice contributes to arthritis development. SKG mice monocolonized with *P copri* developed arthritis after zymosan treatment (Figures 6A and B). The numbers of IL-17⁺ CD4⁺ T cells in the large intestine and popliteal lymph nodes were increased in *P copri*-monocolonized SKG mice after the zymosan injection (Figures 6C and D and Supplementary Figures 12A–D, available on the *Arthritis & Rheumatology* web site at <http://onlinelibrary.wiley.com/doi/10.1002/art.39783/abstract>). We next analyzed whether SKG mouse T cells educated by *P copri*-stimulated DCs are highly pathogenic. Naive splenic T cells from SKG mice cocultured with *P copri*- or *B fragilis*-stimulated DCs for 4 days were adoptively transferred into SCID mice reared in an SPF facility. SKG mouse T cells cocultured with DCs stimulated with either bacterial species induced arthritis upon transfer into SCID mice (Figures 6E and F). However, arthritis development was observed earlier in mice receiving *P copri*-instructed SKG T cells. Thus, SKG mouse T cells are instructed to vigorously respond to arthritis-related autoantigens by *P copri* and possess a heightened ability to induce arthritis.

Finally, we investigated whether SKG mouse T cells activated in the intestine contribute to arthritis development. CD4⁺ T cells were isolated from the large intestine or spleen of SPF-SKG mice and transferred into SCID mice, which were orally treated with antibiotics. Arthritis was induced earlier in SCID mice that had been transferred large intestine CD4⁺ cells than those with spleen T cell transfer (Figures 6G and H). We also analyzed expression

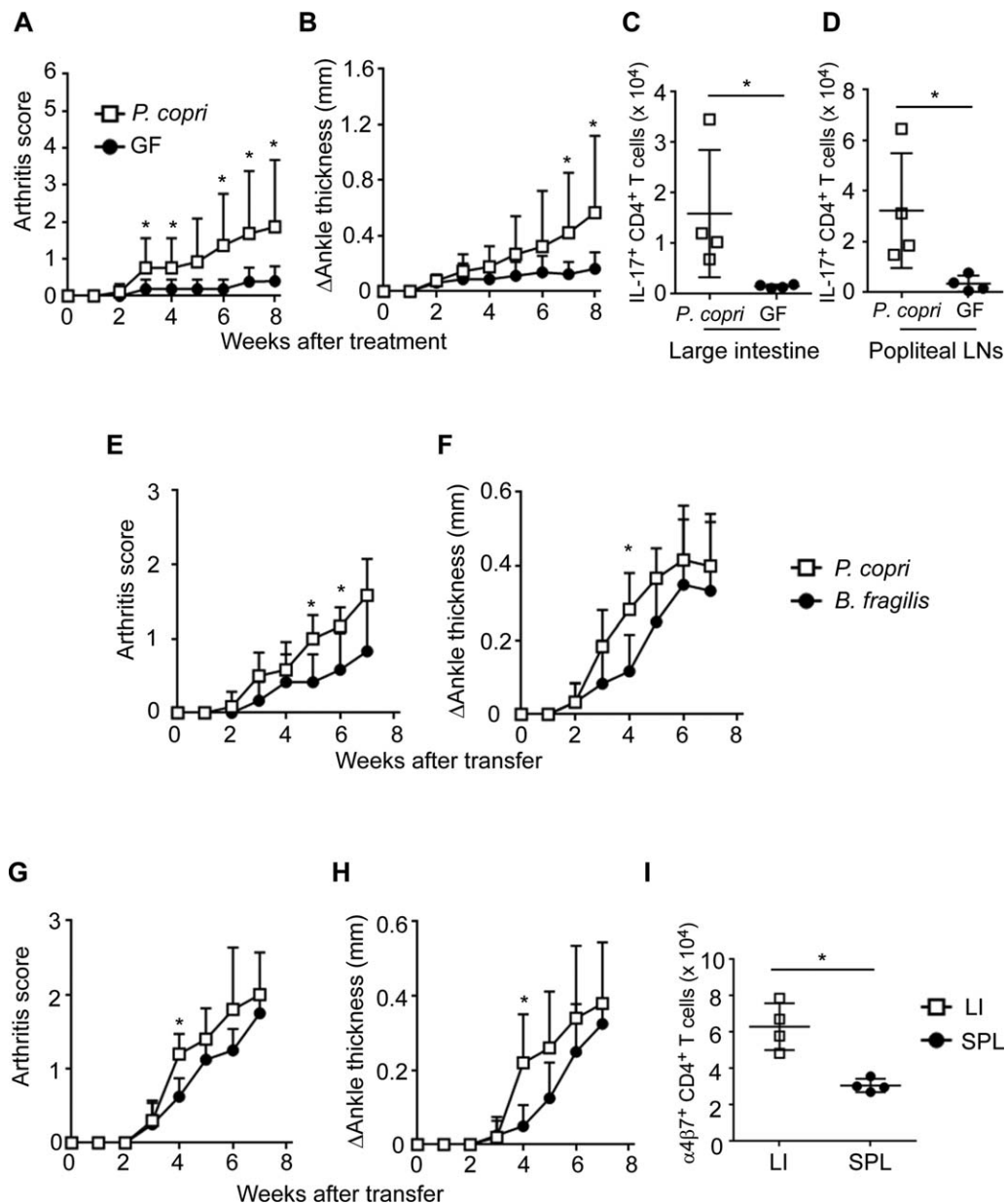


Figure 6. Enhanced Th17 activity in *Prevotella copri*-monocolonized mice. **A–D**, Germ-free (GF) SKG mice were inoculated with or without *P. copri* and then intraperitoneally injected with zymosan. Shown are the arthritis score (**A**) and change in ankle thickness (**B**) in *P. copri*-monocolonized mice ($n = 9$) and germ-free mice ($n = 8$) after injection of zymosan, and the numbers of interleukin-17-positive (IL-17⁺) CD4⁺ T cells in the large intestine (LI) (**C**) and popliteal lymph nodes (LNs) (**D**). **E** and **F**, Naive CD4⁺ T cells from SKG mice were cocultured with dendritic cells that had been stimulated with heat-killed bacteria (*P. copri* or *Bacteroides fragilis* [*B. fragilis*]). Shown are the arthritis score (**E**) and change in ankle thickness (**F**) after the transfer ($n = 6$ mice in each group). **G–I**, CD4⁺ T cells isolated from the large intestine or spleen (SPL) of SKG mice raised in a specific pathogen-free facility were transferred to SCID mice (large intestine, $n = 5$; spleen, $n = 4$). Shown are the arthritis score (**G**) and change in ankle thickness (**H**) after transfer, and the numbers of α 4 β 7⁺ CD4⁺ T cells in the popliteal lymph nodes (**I**). Symbols represent individual mice; bars show the mean \pm SD. * = $P < 0.05$.

of the gut-homing receptor α 4 β 7 on CD4⁺ T cells in the popliteal lymph nodes of these mice. Expression of α 4 β 7 was increased in SCID mice that received CD4⁺ T cells from the large intestine (Figure 6I and Supplementary Figures 13A and B, available on the *Arthritis &*

Rheumatology web site at <http://onlinelibrary.wiley.com/doi/10.1002/art.39783/abstract>). Taken together, these findings suggest that pathogenic T cells were activated in the large intestine and possibly migrated to the joint to induce arthritis.

DISCUSSION

In the current study, we show that dysbiosis in RA patients directly contributes to RA pathogenesis. Similar to the findings in a previous study in a North American population (15), *Prevotella* species, particularly *P copri*, was observed in large abundance within the intestinal microbiota in certain patients with early RA in Japan. Colonization of SKG mice with *Prevotella*-dominated fecal microbiota from RA patients rendered the mice highly susceptible to arthritis. Thus, an altered composition of intestinal microbiota triggered the development of severe joint inflammation.

In SKG mice, in which a missense mutation in *Zap70* resulted in suppression of TCR signaling and defective negative selection, T cells with an autoreactive TCR were generated and contributed to the development of arthritis when stimulated with microbe-activated innate immune cells (8). However, development of arthritis was almost completely blocked by elimination of intestinal microbiota (germ-free condition or antibiotics treatment) in SKG mice. Based on findings in the present study, we propose the following model of pathogenesis of arthritis in SKG mice: T cells with a genetic predisposition for pathogenicity are activated to fully react to arthritis-related autoantigens by *Prevotella*-dominated microbiota in the intestine. Once activated in the intestine, autoreactive T cells induce joint inflammation, possibly by migrating from the intestine into the joints.

Prevotella-dominated RA microbiota, compared with healthy control microbiota, induced severe arthritis in SKG mice. However, the severity of arthritis in SKG mice colonized with human microbiota was milder than that in SKG mice reared under SPF conditions (Maeda Y, et al: unpublished observations). In this regard, it is possible that human microbiota possess more potent regulatory properties that protect the host against arthritis compared with murine microbiota. However, colonization of human microbiota in SKG mice did not increase the number of FoxP3+ regulatory T cells. In addition, the number of IL-17-producing Th17 cells in the large intestine of SKG mice colonized with human microbiota was smaller than that in SPF-housed SKG mice (unpublished observations). Thus, as previously reported (28), human microbiota could not induce development of adaptive immune cells in germ-free mice at a level comparable with that in SPF-housed mice. Therefore, a direct comparison of murine and human microbiota to determine the effect on arthritis would be difficult. *Prevotella*-dominated RA microbiota increased the number of Th17 cells in the large intestine, but not the small intestine, in SKG mice. This might be because *P copri* mainly colonizes in the large intestine and not the small intestine.

SKG mice were originally identified as a mouse model of RA (7). However, subsequent studies have shown that SKG mice could also be used as a model of spondyloarthritis (SpA), because these mice developed spondylitis, ileitis, and uveitis as well as arthritis (9,29,30). In the present study, we did not analyze inflammatory changes in tissue other than joint tissue. It is possible, however, that dysbiosis affects inflammation in the axial joints, gut, and uvea in SKG mice. Thus, it would be an interesting issue in the future to analyze fecal microbiota composition in patients with SpA.

P copri might have an epitope that confers cross-reactivity to arthritis-related autoantigens. However, it is more likely that intestinal DCs stimulated with dysbiotic bacteria activate autoreactive SKG mouse T cells. Indeed, SKG mouse T cells were shown to respond strongly to antigens presented by autologous DCs (24). In addition, microbial stimulation of innate immunity was shown to activate autoreactive SKG mouse T cells that induce arthritis (8). The current study shows that the intestine is a site for the initial T cell activation before the induction of joint inflammation. In this regard, microbiota might be required for the activation of intestinal innate immune cells that in turn stimulate SKG mouse T cells to manifest enhanced autoreactivity.

Prevotella species, which dominates the intestinal microbiota of certain RA patients, has a high capacity to mount Th17-biased innate immune responses. Indeed, the number of innate immune cells possessing a high ability to induce Th17 cell differentiation was increased in the large intestine of RA-SKG mice. Moreover, *P copri* induced production of Th17-related cytokines such as IL-6 and IL-23 at high levels. Thus, the combination of high responsiveness of SKG mouse T cells to DCs and high production of Th17-related cytokines by *P copri*-stimulated DCs might lead to the generation of RPL23A-responsive Th17 cells in mice on the SKG genetic background. Indeed, BALB/c mouse T cells that had been cocultured with *P copri*-stimulated DCs did not produce IL-17 in response to RPL23A. The mechanisms by which *P copri* provokes Th17 responses remains to be elucidated. Conceivably, *P copri* might activate an uncharacterized signaling pathway inducing IL-6 and IL-23.

In the current study, the fecal microbiota of the Japanese population was classified into 4 clusters. The concept of "enterotypes," in which the intestinal microbiota can be clearly classified into 3 types—*Bacteroides*, *Prevotella*, and *Ruminococcus*—has previously been proposed (31). Three clusters, defined as cluster 2, cluster 4, and cluster 1 in this study, were characterized by a high abundance of *Bacteroides*, *Prevotella*, and *Ruminococcus*, respectively. These clusters might correspond to the previously described enterotypes. In rural Africa and tropical Asia, the microbiota contains a high

(>50%) ratio of *Prevotella* species (32,33). It is believed to be attributable to consumption of a diet rich in starch, fiber, and plant polysaccharides but low in animal protein and fat (34,35). However, a high incidence of RA is not reported in these areas. However, *P. copri* used for in vitro experiments in the present study induced enhanced Th17 responses of SKG mouse T cells, although it was not derived from RA patients. Therefore, a precise analysis to compare the microbiota in these populations with those in RA patients in Japan or the US is an important future study.

Given that the dysbiosis in which *Prevotella* species, particularly *P. copri*, is dominant can lead to RA development, it is of note that minocycline is clinically used for the treatment of RA (36,37). Minocycline reportedly possesses several biologic actions other than antimicrobial activity that are effective against autoimmune diseases. These include antiinflammatory and antiapoptotic activities (38). Interestingly, minocycline is effective against *Prevotella* species (39–41); thus, it is possible that the effect of minocycline in RA partly depends on the elimination of *Prevotella* species in the intestine.

Several previous studies in animal models have indicated the involvement of microbiota in RA pathogenesis (10–12). Among these models, germ-free IL-1Ra^{-/-} mice or germ-free K/BxN mice developed arthritis when mono-colonized with *L. bifidus* or SFB, respectively (11,12). However, *Lactobacillus* species is a minor population in the human intestinal microbiota (42), and SFB is not present in the human intestine (43). In sharp contrast, *Prevotella* species is abundantly present in the intestine of certain RA patients. The increase in the number of *Prevotella* species in the intestinal lumen might increase the chance that these bacteria will encounter intestinal innate myeloid cells and T cells, to activate autoreactive T cells. Thus, the intestine is a possible site for the activation of autoreactive T cells essential for the pathogenesis of immune disorders in non-gut tissues.

In this study, we showed that dysbiosis contributes to the development of joint inflammation. When *Prevotella* species predominates in the intestine, autoreactive T cells become highly reactive to autoantigens, including arthritis-related antigens, via activation of innate immunity, among which arthritis-related antigens are included. These T cells can then induce joint inflammation. Recently, several pieces of evidence have demonstrated that the intestine is a site for the development of effector T cells (44,45). Our study indicates that the intestine is also a site for the activation of autoreactive T cells, which induce immune disorders in non-gut tissues. A recent study also demonstrated that autoreactive T cells that induce uveitis are generated in the intestine (46). Several novel approaches directly targeting microbiota (fecal microbiota transplantation in *Clostridium difficile* infection [47]) or microbiota-derived metabolites (inhibition

of intestinal microbial trimethylamine production in atherosclerosis [48]) are being considered for clinical application. Therefore, establishing a strategy to remediate dysbiosis would likely be a beneficial medical intervention to prevent RA disease onset or to maintain the remission state in RA. Thus, more intensive studies enabling us to modify microbial composition in individuals with dysbiosis will be an important issue to be addressed next.

ACKNOWLEDGMENTS

We thank T. Kondo and Y. Magota for providing technical assistance, C. Hidaka for providing secretarial assistance, and S. Pareek for assistance with the use of English. We also thank A. Yura, A. Kitatobe, and other members of the Department of Rheumatology and Allergology, Clinical Research, at National Hospital Organization Osaka Minami Medical Center, as well as K. Maeda and other members of the Division of Allergy, Rheumatology and Connective Tissue Diseases, Department of Internal Medicine, NTT West Osaka Hospital for obtaining fecal samples from the RA patients.

AUTHOR CONTRIBUTIONS

All authors were involved in drafting the article or revising it critically for important intellectual content, and all authors approved the final version to be published. Dr. Takeda had full access to all of the data in the study and takes responsibility for the integrity of the data and the accuracy of the data analysis.

Study conception and design. Maeda, Takeda.

Acquisition of data. Maeda, Kurakawa, Umamoto, Motooka, Ito, Gotoh, Hirota, Matsushita, Furuta, Kayama.

Analysis and interpretation of data. Maeda, Kurakawa, Ito, Hirota, Narazaki, N. Sakaguchi, Nakamura, Iida, Saeki, Kumanogoh, S. Sakaguchi, Takeda.

REFERENCES

- Harris ED Jr. Rheumatoid arthritis. Pathophysiology and implications for therapy. *N Engl J Med* 1990;322:1277–89.
- Cessak G, Kuzawska O, Burda A, Lis K, Wojnar M, Mirowska-Guzel D, et al. TNF inhibitors: mechanisms of action, approved and off-label indications. *Pharmacol Rep* 2014;66:836–44.
- Tanaka T, Narazaki M, Kishimoto T. IL-6 in inflammation, immunity, and disease. *Cold Spring Harb Perspect Biol* 2014;6:a016295.
- Stahl EA, Raychaudhuri S, Remmers EF, Xie G, Eyre S, Thomson BP, et al. Genome-wide association study meta-analysis identifies seven new rheumatoid arthritis risk loci. *Nat Genet* 2010;42:508–14.
- Okada Y, Wu D, Trynka G, Raj T, Terao C, Ikari K, et al. Genetics of rheumatoid arthritis contributes to biology and drug discovery. *Nature* 2014;506:376–81.
- McInnes IB, Schett G. The pathogenesis of rheumatoid arthritis. *N Engl J Med* 2011;365:2205–19.
- Sakaguchi N, Takahashi T, Hata H, Nomura T, Tagami T, Yamazaki S, et al. Altered thymic T-cell selection due to a mutation of the ZAP-70 gene causes autoimmune arthritis in mice. *Nature* 2003;426:454–60.
- Yoshitomi H, Sakaguchi N, Kobayashi K, Brown GD, Tagami T, Sakihama T, et al. A role for fungal β -glucans and their receptor Dectin-1 in the induction of autoimmune arthritis in genetically susceptible mice. *J Exp Med* 2005;201:949–60.
- Rehaume LM, Mondot S, Aguirre de Carcer D, Velasco J, Benham H, Hasnain SZ, et al. ZAP-70 genotype disrupts the relationship

- between microbiota and host, leading to spondyloarthritis and ileitis in SKG mice. *Arthritis Rheumatol* 2014;66:2780–92.
10. Taurog JD, Richardson JA, Croft JT, Simmons WA, Zhou M, Fernandez-Sueiro JL, et al. The germfree state prevents development of gut and joint inflammatory disease in HLA-B27 transgenic rats. *J Exp Med* 1994;180:2359–64.
 11. Abdollahi-Roodsaz S, Joosten LA, Koenders MI, Devesa I, Roelofs MF, Radstake TR, et al. Stimulation of TLR2 and TLR4 differentially skews the balance of T cells in a mouse model of arthritis. *J Clin Invest* 2008;118:205–16.
 12. Wu HJ, Ivanov II, Darce J, Hattori K, Shima T, Umesaki Y, et al. Gut-residing segmented filamentous bacteria drive autoimmune arthritis via T helper 17 cells. *Immunity* 2010;32:815–27.
 13. Vahtovuo J, Munukka E, Korkeamaki M, Luukkainen R, Toivanen P. Fecal microbiota in early rheumatoid arthritis. *J Rheumatol* 2008;35:1500–5.
 14. Zhang X, Zhang D, Jia H, Feng Q, Wang D, Liang D, et al. The oral and gut microbiomes are perturbed in rheumatoid arthritis and partly normalized after treatment. *Nat Med* 2015;21:895–905.
 15. Scher JU, Sczesnak A, Longman RS, Segata N, Ubeda C, Bielski C, et al. Expansion of intestinal *Prevotella copri* correlates with enhanced susceptibility to arthritis. *Elife* 2013;2:e01202.
 16. Belkaid Y, Hand TW. Role of the microbiota in immunity and inflammation. *Cell* 2014;157:121–41.
 17. Aletaha D, Neogi T, Silman AJ, Funovits J, Felson DT, Bingham CO 3rd, et al. 2010 Rheumatoid arthritis classification criteria: an American College of Rheumatology/European League Against Rheumatism collaborative initiative. *Arthritis Rheum* 2010;62:2569–81.
 18. Matsuki T, Watanabe K, Fujimoto J, Kado Y, Takada T, Matsumoto K, et al. Quantitative PCR with 16S rRNA-gene-targeted species-specific primers for analysis of human intestinal bifidobacteria. *Appl Environ Microbiol* 2004;70:167–73.
 19. Andersson AF, Lindberg M, Jakobsson H, Backhed F, Nyren P, Engstrand L. Comparative analysis of human gut microbiota by barcoded pyrosequencing. *PLoS One* 2008;3:e2836.
 20. Edgar RC. Search and clustering orders of magnitude faster than BLAST. *Bioinformatics* 2010;26:2460–1.
 21. Cole JR, Chai B, Farris RJ, Wang Q, Kulam-Syed-Mohideen AS, McGarrell DM, et al. The ribosomal database project (RDP-II): introducing myRDP space and quality controlled public data. *Nucleic Acids Res* 2007;35(Database issue):D169–72.
 22. Quast C, Pruesse E, Yilmaz P, Gerken J, Schweer T, Yarza P, et al. The SILVA ribosomal RNA gene database project: improved data processing and web-based tools. *Nucleic Acids Res* 2013;41(Database issue):D590–6.
 23. Matsuki T, Watanabe K, Fujimoto J, Miyamoto Y, Takada T, Matsumoto K, et al. Development of 16S rRNA-gene-targeted group-specific primers for the detection and identification of predominant bacteria in human feces. *Appl Environ Microbiol* 2002;68:5445–51.
 24. Hirota K, Hashimoto M, Yoshitomi H, Tanaka S, Nomura T, Yamaguchi T, et al. T cell self-reactivity forms a cytokine milieu for spontaneous development of IL-17(+) Th cells that cause autoimmune arthritis. *J Exp Med* 2007;204:41–7.
 25. Atarashi K, Nishimura J, Shima T, Umesaki Y, Yamamoto M, Onoue M, et al. ATP drives lamina propria T(H)17 cell differentiation. *Nature* 2008;455:808–12.
 26. Ito Y, Hashimoto M, Hirota K, Ohkura N, Morikawa H, Nishikawa H, et al. Detection of T cell responses to a ubiquitous cellular protein in autoimmune disease. *Science* 2014;346:363–8.
 27. Denning TL, Wang YC, Patel SR, Williams IR, Pulendran B. Lamina propria macrophages and dendritic cells differentially induce regulatory and interleukin 17-producing T cell responses. *Nat Immunol* 2007;8:1086–94.
 28. Chung H, Pamp SJ, Hill JA, Surana NK, Edelman SM, Troy EB, et al. Gut immune maturation depends on colonization with a host-specific microbiota. *Cell* 2012;149:1578–93.
 29. Benham H, Rehaume LM, Hasnain SZ, Velasco J, Baillet AC, Ruutu M, et al. Interleukin-23 mediates the intestinal response to microbial β -1,3-glucan and the development of spondyloarthritis pathology in SKG mice. *Arthritis Rheumatol* 2014;66:1755–67.
 30. Ruutu M, Thomas G, Steck R, Degli-Esposti MA, Zinkernagel MS, Alexander K, et al. β -glucan triggers spondylarthritis and Crohn's disease-like ileitis in SKG mice. *Arthritis Rheum* 2012;64:2211–22.
 31. Arumugam M, Raes J, Pelletier E, Le Paslier D, Yamada T, Mende DR, et al. Enterotypes of the human gut microbiome. *Nature* 2011;473:174–80.
 32. De Filippo C, Cavalieri D, Di Paola M, Ramazzotti M, Poullet JB, Massart S, et al. Impact of diet in shaping gut microbiota revealed by a comparative study in children from Europe and rural Africa. *Proc Natl Acad Sci U S A* 2010;107:14691–6.
 33. Nakayama J, Watanabe K, Jiang J, Matsuda K, Chao SH, Haryono P, et al. Diversity in gut bacterial community of school-age children in Asia. *Sci Rep* 2015;5:8397.
 34. Wu GD, Chen J, Hoffmann C, Bittinger K, Chen YY, Keilbaugh SA, et al. Linking long-term dietary patterns with gut microbial enterotypes. *Science* 2011;334:105–8.
 35. Kovatcheva-Datchary P, Nilsson A, Akrami R, Lee YS, De Vadder F, Arora T, et al. Dietary fiber-induced improvement in glucose metabolism is associated with increased abundance of *Prevotella*. *Cell Metab* 2015;22:971–82.
 36. Tilley BC, Alarcon GS, Heyse SP, Trentham DE, Neuner R, Kaplan DA, et al. Minocycline in rheumatoid arthritis: a 48-week, double-blind, placebo-controlled trial. MIRA Trial Group. *Ann Intern Med* 1995;122:81–9.
 37. O'Dell JR, Blakely KW, Mallek JA, Eckhoff PJ, Leff RD, Wees SJ, et al. Treatment of early seropositive rheumatoid arthritis: a two-year, double-blind comparison of minocycline and hydroxychloroquine. *Arthritis Rheum* 2001;44:2235–41.
 38. Garrido-Mesa N, Zarzuelo A, Galvez J. Minocycline: far beyond an antibiotic. *Br J Pharmacol* 2013;169:337–52.
 39. Jones AA, Kornman KS, Newbold DA, Manwell MA. Clinical and microbiological effects of controlled-release locally delivered minocycline in periodontitis. *J Periodontol* 1994;65:1058–66.
 40. Van Steenberghe D, Bercy P, Kohl J, De Boever J, Adriaens P, Vanderfaeillie A, et al. Subgingival minocycline hydrochloride ointment in moderate to severe chronic adult periodontitis: a randomized, double-blind, vehicle-controlled, multicenter study. *J Periodontol* 1993;64:637–44.
 41. Takahashi N, Ishihara K, Kimizuka R, Okuda K, Kato T. The effects of tetracycline, minocycline, doxycycline and ofloxacin on *Prevotella intermedia* biofilm. *Oral Microbiol Immunol* 2006;21:366–71.
 42. Matsuda K, Tsuji H, Asahara T, Matsumoto K, Takada T, Nomoto K. Establishment of an analytical system for the human fecal microbiota, based on reverse transcription-quantitative PCR targeting of multicopy rRNA molecules. *Appl Environ Microbiol* 2009;75:1961–9.
 43. Prakash T, Oshima K, Morita H, Fukuda S, Imaoka A, Kumar N, et al. Complete genome sequences of rat and mouse segmented filamentous bacteria, a potent inducer of Th17 cell differentiation. *Cell Host Microbe* 2011;10:273–84.
 44. Hooper LV, Littman DR, Macpherson AJ. Interactions between the microbiota and the immune system. *Science* 2012;336:1268–73.
 45. Littman DR, Pamer EG. Role of the commensal microbiota in normal and pathogenic host immune responses. *Cell Host Microbe* 2011;10:311–23.
 46. Horai R, Zarate-Blades CR, Dillenburg-Pilla P, Chen J, Kielczewski JL, Silver PB, et al. Microbiota-dependent activation of an autoreactive T cell receptor provokes autoimmunity in an immunologically privileged site. *Immunity* 2015;43:343–53.
 47. Van Nood E, Vrieze A, Nieuwdorp M, Fuentes S, Zoetendal EG, de Vos WM, et al. Duodenal infusion of donor feces for recurrent *Clostridium difficile*. *N Engl J Med* 2013;368:407–15.
 48. Wang Z, Roberts AB, Buffa JA, Levison BS, Zhu W, Org E, et al. Non-lethal inhibition of gut microbial trimethylamine production for the treatment of atherosclerosis. *Cell* 2015;163:1585–95.